Title
White matter microstructural correlates of associative learning in the oldest-old

Journal
Cognitive, Affective, & Behavioral Neuroscience, 23(1)

ISSN
1530-7026

Authors
Merenstein, Jenna L
Corrada, María M
Kawas, Claudia H
et al.

Publication Date
2023-02-01

DOI
10.3758/s13415-022-01035-7

Cognitive, Affective, & Behavioral Neuroscience
https://doi.org/10.3758/s13415-022-01035-7

RESEARCH ARTICLE

White matter microstructural correlates of associative learning in the oldest-old

Jenna L. Merenstein[1,2] · **María M. Corrada**[3,4,5] · **Claudia H. Kawas**[3,4,6] · **Ilana J. Bennett**[1]

Accepted: 9 September 2022

Abstract

The ability to learn associations between events is critical for everyday functioning (e.g., decision making, social interactions) and has been attributed to structural differences in white matter tracts connecting cortical regions to the hippocampus (e.g., fornix) and striatum (e.g., internal capsule) in younger-old adults (ages 65-85 years). However, evidence of associative learning has not been assessed within oldest-old adults (ages 90+ years), despite its relevance to other extensively characterized cognitive abilities in the oldest-old and the relatively large effect of advanced age on the microstructural composition of these white matter tracts. We acquired multicompartment diffusion-weighted magnetic resonance imaging data from 22 oldest-old adults without dementia (mean age = 92.91 ± 1.44 years) who also completed an associative learning task. Behavioral results revealed significantly better associative learning performance during later task stages, as expected if participants incidentally learned the cue-cue-target associations for frequently occurring event triplets. Moreover, better learning performance was significantly predicted by better microstructure of cortico-striatal white matter (posterior limb of the internal capsule). Finding that associative learning abilities in the 10th decade of life are supported by better microstructure of white matter tracts connecting the cortex to the striatum underscores their importance to learning performance across the entire lifespan.

Keywords Nonagenarians · Diffusion imaging · Associative learning · White matter · Individual differences

The ability to form associations between events, even when their relationship cannot be described, is crucial for learning higher-order skills ranging from using new technology to communicating using nonverbal cues (Lieberman, 2000; Seger, 1994)—abilities that help us adapt to and interact with the environment throughout our life. In the laboratory, behavioral evidence of implicit associative learning (IAL) is seen as faster or more accurate responses to stimuli that can be predicted based on their relationship to prior events. In the Triplet Learning Task (TLT; J. H. Howard et al., 2008), for example, participants respond faster and more accurately to the location of a target that can be predicted by the location of two cue events when the cue-cue-target association (or "triplet") occurs more frequently. Using the TLT, as well as other learning paradigms, IAL has been established in adults across most of the lifespan, albeit with smaller learning effects in younger-old (65-85 years) relative to young (20-30 years) adults (Bennett et al., 2007; Curran, 1997; Howard et al., 2008; Howard & Howard, 2013; Howard et al., 2004; Seaman et al., 2014; Simon et al., 2010, 2012; Stillman, Howard, et al., 2016a; Stillman, You, et al., 2016c). But IAL has not yet been demonstrated in oldest-old adults (90+ years) despite extensive characterization of their performance across other cognitive domains (Melikyan et al., 2019), some of which likely rely on IAL (e.g., episodic memory, executive control; Merenstein & Bennett, 2022).

In addition to age group differences, prior IAL work has revealed individual differences in performance within each age group such that some individuals learn better than their

✉ Jenna L. Merenstein
jenna.merenstein@duke.edu

1 Department of Psychology, University of California, Riverside, CA, USA

2 Brain Imaging and Analysis Center, Duke University, Box 3918, Durham, NC 27710, USA

3 Institute for Memory Impairments and Neurological Disorders, University of California, Irvine, CA, USA

4 Department of Neurology, University of California, Irvine, CA, USA

5 Department of Epidemiology, University of California, Irvine, CA, USA

6 Department of Neurobiology and Behavior, University of California, Irvine, CA, USA

Published online: 26 September 2022

peers (Bennett et al., 2011; Franco et al., 2021; Rieckmann et al., 2010). As in younger-old adults, individual differences in IAL within oldest-old adults may be due to differences in the properties of white matter tissue connecting brain regions involved in learning, which can be measured using diffusion-weighted magnetic resonance imaging (MRI). For example, previous diffusion work from our group found that IAL performance in healthy younger-old adults was associated with microstructure of white matter tracts connecting the hippocampus and dorsal striatum to the frontal and motor cortices (Bennett et al., 2011), regions that have been implicated in IAL tasks by functional MRI studies (Dennis & Cabeza, 2011; Merenstein, Petok, et al., 2021b; Rieckmann et al., 2010; Simon et al., 2012). These same cortico-hippocampal (e.g., fornix) and cortico-striatal (e.g., internal capsule) white matter tracts exhibit accelerated microstructural declines in advanced age (Merenstein, Corrada, et al., 2021a). IAL therefore may be impaired in at least some oldest-old adults due to degradation of white matter that connects brain regions involved in learning. This may drive individual differences in IAL such that some oldest-old adults with worse microstructure in these regions may show worse IAL, whereas oldest-old adults with better microstructure should exhibit better IAL performance.

Prior IAL work has also revealed that learning effects are sometimes larger for one dependent measure relative to the other. For example, in younger age groups, a significant difference in performance to high- and low-frequency events is sometimes seen for reaction time but not accuracy (Merenstein, Petok, et al., 2021b; Simon et al., 2012; Stillman, Howard, et al., 2016a; Stillman, You, et al., 2016c), whereas other studies observe significant evidence of IAL for both measures (Bennett et al., 2011; Howard et al., 2008). If these learning effects are more subtle in the oldest-old, it may be advantageous to assess IAL in a way that takes performance on both dependent measures into account. One such approach is rank-ordering binning metrics (Draheim et al., 2016; Hughes et al., 2014), in which better (lower) scores indicate that a participant responded faster to accurate high-frequency than low-frequency triplets and had fewer inaccurate responses to high-frequency triplets.

We assessed IAL in nonagenarians for the first time and tested whether IAL performance was related to individual differences in its microstructural substrates. Oldest-old adults without dementia, including cognitively normal individuals and those diagnosed with cognitive impairment no dementia (CIND), performed a version of the TLT. Diffusion-weighted MRI data was also acquired and multicompartment diffusion metrics (i.e., neurite orientation density and dispersion imaging, NODDI; Zhang et al., 2012) were extracted from the fornix and internal capsule. Analyses first examined whether oldest-old adults exhibited behavioral evidence of IAL using a rank-ordering binning learning metric. We then assessed whether individual differences in white matter microstructure predicted IAL performance. Based on our previous observation of positive relations between IAL performance and diffusion tensor imaging measures of cortico-hippocampal and cortico-striatal microstructure in younger-old adults (Bennett et al., 2011), we hypothesized that better IAL performance also would be associated with better white matter microstructure in similar regions (i.e., fornix, internal capsule) in the oldest-old.

Method

Participants

We recruited 28 oldest-old adults (90-98 years, 11 males) who were current participants in The 90+ Study, a longitudinal study of aging and dementia in the oldest-old (see Kawas and Corrada, 2006 for additional details), who had not previously received a diagnosis of dementia. These individuals were clinically diagnosed as cognitively normal (n = 19) or cognitively impaired no dementia (CIND; n = 9), the latter of which captures individuals with cognitive or functional losses that were not of sufficient severity to meet the Diagnostic and Statistical Manual of Mental Disorders, 4th edition criteria for dementia (del Barrio, 2004; Graham et al., 1997). Diagnoses were based on thorough neurological, physical, and neuropsychological evaluations by trained examiners at their biannual visit closest to the MRI testing session. The cognitive status was missing for one participant who was included in the CIND group, because they scored 25 on the Mini Mental State Examination (MMSE; Folstein et al., 1975).

Participants were screened for conditions that would prevent them from being able to enter the MRI scanner (e.g., having ferrous metal implants). We excluded one cognitively normal participant for having a cortical mass that covered large portions of white matter. Using a cutoff of four standard deviations below the mean of the sample, four additional participants (n = 3 cognitively normal, n = 1 CIND) were excluded for responding to too few trials (<42.7% of all trials), and one participant with CIND was excluded for poor task performance (accuracy < 42.6%). These six individuals were excluded from all behavioral and imaging data analyses. The final sample was 22 individuals (mean age = 92.91 ± 1.44; 64% females; 95% white; 9% Hispanic; mean years of education = 15.55 ± 2.89; mean MMSE score out of 30 = 26.18 ± 2.86).

This study was conducted in compliance with the Institutional Review Boards for the University of California, Irvine, and Riverside. Each participant provided informed consent and was compensated for their participation.

Triplet learning task

Task design Participants completed an abbreviated, deterministic version of an implicit associative learning task (triplet learning task, TLT; Franco et al., 2021; Merenstein, Petok, et al., 2021b) at their personal residences on a Surface Pro tablet. In the TLT, participants viewed four open circles presented in a row on a white background (Fig. 1). Each trial, or "triplet," consisted of a cue-cue-target sequence (2,850 ms total) in which two "cue" circles filled in red (260 ms each) followed by one "target" circle filling in green (1,000 ms), with interstimulus intervals of 340 ms and intertrial intervals of 650 ms. Relative to our previous work using this version of the TLT (150-ms cue, 800-ms target, 150-ms ISI, 600-ms ITI, and 2,000-ms total trial durations (Franco et al., 2021; Merenstein, Petok, et al., 2021b), stimuli and intervals were presented at a slower rate for this advanced age group. Participants passively viewed the red cues and were told to respond as quickly and accurately as possible to the location of the green target via the corresponding keyboard response. The total time required to complete the task was 22.8 minutes.

Critically, the locations of the red cues could be used to predict the location of the green target, with some triplets occurring more versus less frequently. Twelve unique triplets were randomly selected from the 64 possible cue-cue-target combinations, after excluding 40 triplets that had any two events in the same location (e.g., 111, 112, 121; where the number corresponds to the location of the four circles on the screen from left to right) as their performance reflects preexisting response tendencies (Boyer, Destrebecqz, & Cleeremans, 2005; Howard et al., 2008), and after counterbalancing to ensure that cues and targets occurred in each location equally often. Within each block, four triplets were each presented six times (high frequency [HF]; 75% of trials) and eight triplets were each presented once (low frequency [LF]; 25% of trials). All participants completed a total of fifteen 32-trial blocks, which were equally divided into five task stages. To prevent fatigue, a self-paced break was provided after each block.

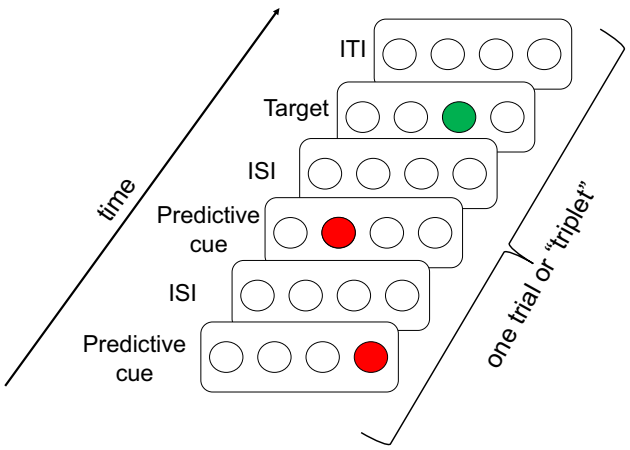

Fig. 1 Visualization of an example trial on the Triplet Learning Task (TLT). Each trial, or "triplet," consists of a sequential presentation of two red cue circles followed by a green target circle. Participants passively view the location of the first two red cues of each triplet and respond only to the location of the green target via the corresponding keyboard button. Evidence of associative learning is seen when participants respond faster or more accurately to triplets that are presented more (75% of the time; high frequency) versus less (25% of the time; low frequency) often. ISI = interstimulus interval; ITI = intertrial interval

Associative learning measure Accuracy and reaction times were recorded on each trial for each HF or LF triplet type. To obtain a measure of IAL, we calculated a rank-ordering binning learning metric that combined the accuracy and reaction time measures (Draheim et al., 2016; Hughes et al., 2014). The first step, which was performed once across all 480 trials (i.e., all blocks and task stages) but separately within each participant, involved calculating the average reaction time to all accurate LF triplets and subtracting that value from their reaction time to each accurate HF triplet (120 possible accurate HF trials). This yielded difference scores in which lower values indicate that participants responded faster to that particular HF triplet than their response to the average LF triplet (i.e., better learning). Inaccurate HF triplet, LF triplet, and no response trials were not given a value at this step. The next step, which was performed across all accurate HF trials for all participants (7,920 possible accurate HF trials), involved rank ordering the difference scores into deciles and assigning each score a decile value ranging from 1 (best performance) to 10 (worst performance). Separately from the decile value calculations, inaccurate HF triplet trials were assigned a value of 20 as a penalty (Draheim et al., 2016). Finally, a bin score was computed separately for each task stage and each participant by summing the respective decile and penalty values.

Recognition task A subset of participants (n = 12 cognitively normal, n = 5 CIND) also completed a subsequent computer-based recognition task to test for awareness of the frequently occurring cue-cue-target associations (Franco et al., 2021; Merenstein, Petok, et al., 2021b). Participants indicated via keyboard responses whether a series of HF, LF, or never presented (no frequency, NF) triplets occurred "frequently," "infrequently," or "not at all" during the previously completed version of the TLT. Mean accuracy to each triplet type was calculated separately for each participant.

Imaging data

Acquisition Before behavioral testing, participants underwent a structural imaging protocol at the University of

California, Irvine Facility for Imaging and Brain Research (interval range 8–29 days, except for 2 individuals up to 81 days). Imaging data were acquired using a 3T Siemens Prisma MRI scanner fitted with a 32-channel head coil.

A single, high-resolution, T1-weighted image (magnetization-prepared rapid gradient-echo sequence, MP-RAGE) was acquired with the following parameters: echo time (TE) / repetition time (TR) = 2.72 / 2,400 ms, field of view (FOV) = 256 × 256 × 192 mm, matrix size = 320 x 320 x 240, voxel size = 0.8 mm^3, Generalized Autocalibrating Partially Parallel Acquisitions (GRAPPA) acceleration factor = 2, 208 axial slices, and scan time = 6:28.

A single, diffusion-weighted, single-shot, spin-echo, echo planar imaging image was acquired with the following parameters: TE / TR = 102 / 3,500 ms, FOV = 212 × 182 mm^2, matrix size = 128 × 110, voxel size = 1.7 mm^3, multiband factor = 4, 64 slices with no gap, and scan time = 16:12. Bipolar diffusion-weighting gradients were applied in 64 directions with *b* values of 1500 s/mm^2 and 3000 s/mm^2 with 3 $b = 0$ images.

Processing For each participant, diffusion data were preprocessed using AFNI (Analysis of Functional NeuroImages; Cox, 1996) to remove nonbrain tissue and generate a whole-brain mask, FSL (FMRIB's Software Library, www.fmrib.ox.ac.uk/fsl) to correct for head movement and eddy-current induced distortions (EDDY), and the NODDI MATLAB toolbox (https://www.nitrc.org/projects/noddi_toolbox) to obtain diffusion estimates. NODDI provides measures of free diffusion (also known as fraction of isotropic diffusion [FISO]), intracellular diffusion (also known as intracellular volume fraction[FICVF] or neurite density index [NDI]), and dispersed diffusion (also known as orientation dispersion index [ODI]) modeled as an isotropic sphere, sticks, and dispersion of the sticks, respectively (Zhang et al., 2012). An increase in the free diffusion measure indicates that there is a reduction in neural tissue that allows molecular water to diffuse freely in all direction (e.g., neurodegeneration, increased Virchow Robin perivascular spaces), an increase in intracellular diffusion indicates that more molecular water is highly restricted within neural tissue (e.g., inflammation, myelin ballooning or splitting myelin sheaths), and an increase in dispersed diffusion indicates that intracellular diffusion is less directionally homogeneous (e.g., reduced coherence of fiber orientation) (Garcia-Hernandez et al., 2022; Sato et al., 2017; Yi et al., 2019).

Regions of interest Based on known anatomical connections from the hippocampus and dorsal striatum to the prefrontal or motor cortices (Wakana et al., 2004; Wycoco et al., 2013), we created standard masks of the fornix (body and bilatersal cres) from FSL's Fornix_FMRIB_FA1mm mask (Brown et al., 2017) and the bilateral anterior and posterior limbs of the internal capsule and the thalamic radiations (for a control region) from the JHU ICBM-labels-1mm white matter atlas (Mori et al., 2008). We used a standard region of interest approach to allow for more reproducible measures from each region in each participant and because tractography would be difficult in this age group due to their extensive white matter disease (which we accounted for by limiting analyses to normal appearing white matter, see below) and gray matter atrophy (which would lead to smaller seed/target regions). A visualization of these tracts overlaid on a standard white matter template is provided in Fig. 2.

For each participant, these standard white matter masks were aligned to native diffusion space using the following registration

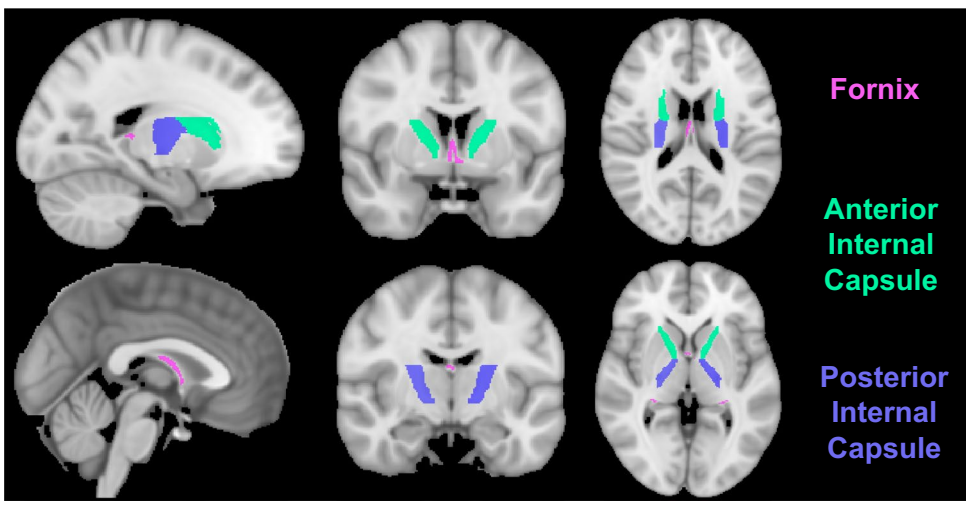

Fig. 2 Standard regions of interest. Masks of the fornix from FSL (pink) and the anterior (green) and posterior (blue) limbs of the internal capsule from the John Hopkins University (JHU) standard atlas are overlaid on a standard Montreal Neurological Institute (MNI) 152 brain with 1mm^3 resolution and thresholded by a white matter segmentation mask (partial volume estimate > 0.50)

steps: (1) alignment of the MP-RAGE image to the Montreal Neurological Institute (MNI) 152 1-mm resolution standard image using an affine transformation with 12 degrees of freedom, (2) alignment of the diffusion image with no diffusion weighting applied (i.e., dtifit_s0) to the MP-RAGE image using a boundary-based registration with six degrees of freedom, (3) concatenation of the diffusion to MP-RAGE and MP-RAGE to MNI transformations, (4) inverting this concatenated transformation, and (5) applying the inverted transformation to align the standard JHU ICBM white matter masks to native diffusion space. The boundary-based registration is based on white matter boundaries that exhibit more reliable age-related changes in signal intensity than gray matter tissue and is therefore fairly robust to pathologies and artifacts seen in diffusion images (Greve & Fischl, 2009), which is especially important in advanced age. In addition, a trained researcher that was blinded to cognitive status visually inspected the quality of alignments and mask coverage for all three regions of interest, confirming that all masks were of usable quality.

Each region of interest was limited to normal appearing white matter. For each participant, a white matter mask that excludes hyperintense tissue was generated on their MP-RAGE image via FSL's Automated Segmentation Tool (FAST; Zhang et al., 2001), which classifies white matter hyperintensities as either gray matter or cerebrospinal fluid due to their low-intensity values (Melazzini et al., 2021). The partial volume estimate of this white matter mask was thresholded at 0.5, aligned to diffusion space by applying the inversion of the diffusion to MP-RAGE transformation described above, and multiplied by each region of interest mask.

Before extracting diffusion metrics, the region of interest masks were further limited to voxels with restricted diffusion below 0.99 to account for artifactual, mathematical errors in regions with insufficient signal (Emmenegger et al., 2021). For each participant, the resulting masks were then separately multiplied by each diffusion metric image (free, intracellular, and dispersed), and values were averaged across voxels within each mask.

Statistical analyses To test for behavioral evidence of IAL, we conducted a repeated measures analysis of variance (ANOVA) with Task Stage (1-5) as a within-person variable and bin scores as the dependent variable. To test for potential effects of demographic variables and cognitive status on IAL performance, we also conducted an analysis of covariance (ANCOVA) with Task Stage (1-5) as a within-person variable, bin scores as the dependent variable, and sex (dummy coded as 0 for female and 1 for male) and years of education completed as covariates.

To test whether participants could accurately indicate whether some triplets occurred more often, separate two-sided one-sample *t*-tests compared mean recognition accuracy to each Triplet Type (HF, LF, NF) to chance (0.33).

Finally, to test whether white matter microstructure predicted IAL performance, we conducted multiple linear regression models with the average diffusion estimates from each region of interest (fornix and bilateral anterior and posterior limbs of the internal capsule) as simultaneous predictors of IAL performance, with separate models for each diffusion metric (free, intracellular, and dispersed). Because there was better IAL performance during task stages 2-5 relative to task stage 1 (see *Results*), the outcome variable was limited to average IAL bin scores across task stages 2-5. To test for potential effects of demographic variables on the relation between white matter microstructure and IAL performance, we repeated these regression models with the addition of sex and years of education as predictor variables. Finally, to test the specificity of our findings, we also repeated these regression models with the addition of the thalamic radiation control tract. Analyses were conducted using a combination of SPSS Version 26 and R-Studio Version 1.1.442.

Power analyses A series of power analyses conducted using G-Power (Faul et al., 2007) confirmed that our sample was sufficiently large enough to identify significant IAL effects and relations between IAL and white matter microstructure. For the ANOVA, we used values from our recent work observing IAL as a significant Triplet Type by Learning Stage interaction for reaction time across 36 younger and 26 younger-old (ages 65-87) adults, $F(1, 59) = 18.60$, $p < 0.001$, $\eta_p^2 = 0.24$ (Franco et al., 2021). Using this effect size revealed that the current study required a sample size of eight participants to detect a comparable effect with a single group, five repeated measurements, alpha = 0.05, and power = 0.962.

For the linear regressions, we based our power analysis on the same study, which observed significant relations between performance on the TLT and NODDI measurements of gray matter microstructure in a sample of 26 younger-old adults (Franco et al., 2021). This analysis revealed that a minimum sample of 24 participants was required to detect significant two-tailed effects with an effect size = 0.516, alpha = 0.05, and power = 0.809. Because NODDI gray matter effect sizes may not necessarily generalize to white matter, we repeated this power analysis using values from our earlier study finding significant relations between IAL and diffusion tensor imaging estimates of fractional anisotropy in 14 younger-old adults (ages 63-72 years; Bennett et al., 2011). This analysis revealed that a minimum sample of 15 participants was required to detect significant two-tailed effects with an effect size = 0.620, alpha = 0.05, and power = 0.816.

Results

Associative learning performance

Evidence of IAL was assessed using a repeated measures ANOVA with Task Stage (1-5) as a within-person variable

and bin scores as the dependent variable. Results revealed a significant main effect of Task Stage, $F(4, 84) = 9.99$, $p < 0.001$ (Fig. 3), with significantly worse performance seen as higher bin scores for Task Stage 1 (mean = 720.50 ± 204.12) relative to Task Stage 2 (mean = 594.86 ± 112.50; difference = 125.64 ± 153.68), $t(21) = 3.834$, $p = 0.001$, Stage 3 (mean = 589.68 ± 111.26; difference = 130.82 ± 166.02), $t(21) = 3.696$, $p = 0.001$, Stage 4 (mean = 586.82 ± 109.14; difference = 133.68 ± 169.73), $t(21) = 3.694$, $p = 0.001$, and Stage 5 (mean = 599.96 ± 125.76; difference = 120.55 ± 183.81), $t(21) = 3.076$, $p = 0.006$. There were no significant differences in bin scores observed among the latter four stages, ps > 0.271. Results for the traditional accuracy and reaction time measures are provided in the Supplementary Material, where similar, but less sensitive, evidence of IAL was seen for accuracy.

We also performed a series of robustness checks for the reliability of our bin score measurement by performing the calculations in separate halves of the sample and with alternate penalty scores (Supplementary Material). In each case, results revealed significant evidence of IAL.

Effect of demographic variables When repeating the above analysis as an ANCOVA with sex and years of education as covariates, the main effect of Task Stage remained significant, $F(4, 76) = 11.24$, $p < 0.001$, but there were no significant main effects of or interactions with sex and education, ps > 0.383.

Awareness of the regularity To assess whether participants could accurately indicate whether some triplets occurred more often, separate two-sided one-sample t-tests compared mean recognition accuracy to each Triplet Type (HF, LF, NF) to chance (0.33). Results revealed that accuracy to HF (mean = 0.47 ± 0.08), LF (mean = 0.27 ± 0.06), and NF (mean = 0.40 ± 0.07) triplets did not significantly differ from chance, ps > 0.097. These results provide confidence that participants were not aware of the regularities learned here.

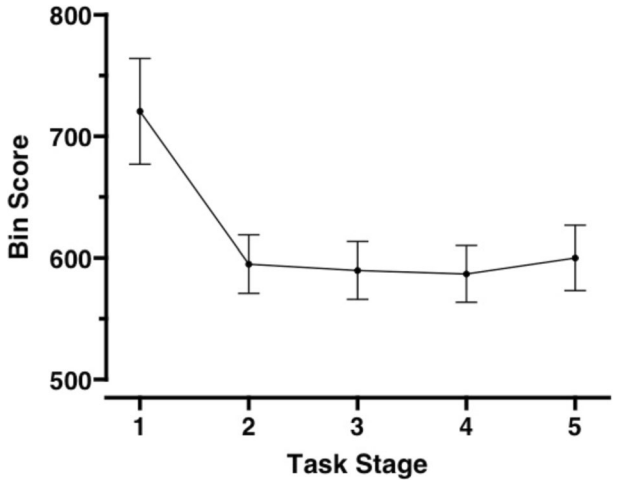

Fig. 3 Associative learning performance. Behavioral results are displayed as a function of Task Stage, with evidence of implicit associative learning observed as significantly lower bin scores for Stages 2 through 5 compared with Stage 1. Error bars represent standard error of the mean

Associative learning relates to white matter microstructure

We conducted multiple linear regression models with white matter microstructure estimates from each region of interest (fornix, anterior limb of the internal capsule, posterior limb of the internal capsule) as simultaneous predictors of IAL performance (average IAL bin score), separately for each diffusion metric (free, intracellular, and dispersed diffusion).

The models predicting IAL performance using the dispersed, $R^2 = 0.38$, $F(3, 18) = 3.71$, $p = 0.031$, and free, $R^2 = 0.33$, $F(3, 18) = 2.95$, $p = 0.060$, but not restricted, $R^2 = 0.11$, $F(3, 18) = 0.73$, $p = 0.548$, diffusion metrics were significant or trending. When examining the individual predictor variables, we found that better learning performance (lower bin scores) was significantly associated with lower dispersed, $\beta = 0.66$, $t(21) = 3.26$, $p = 0.004$, and free, $\beta = 0.54$, $t(21) = 2.39$, $p = 0.028$, diffusion in the posterior limb of the internal capsule (Fig. 4). None of diffusion metrics in the fornix and anterior limb of the internal capsule were significant predictors of IAL performance (Table 1). Multiple regression models with white matter microstructure estimates predicting traditional accuracy measures of IAL (i.e., the difference between HF and LF triplets) were not significant, ps > 0.201.

Of note, dispersed and free diffusion in the posterior limb of the internal capsule also remained a significant predictor of IAL after modeling the interim interval between MRI and behavioral testing as a covariate, ps < 0.030. Dispersed, $\beta = 0.78$, $t(21) = 3.05$, $p = 0.011$, but not free, $p = 0.126$, diffusion in the posterior limb of the internal capsule also remained a significant predictor of IAL when limiting analyses to the 15 participants with normal cognition, suggesting that these effects were not solely driven by the 7 participants with CIND.

Effect of demographic variables When repeating these multiple regression models with the addition of sex and years of education as predictors, the pattern of results did not change (Supplementary Table 2).

Control tract When repeating these multiple regression models with microstructure of the thalamic radiations as an additional variable, we observed no significant effect of thalamic radiation microstructure on IAL performance for any of the diffusion metrics, ps > 0.380.

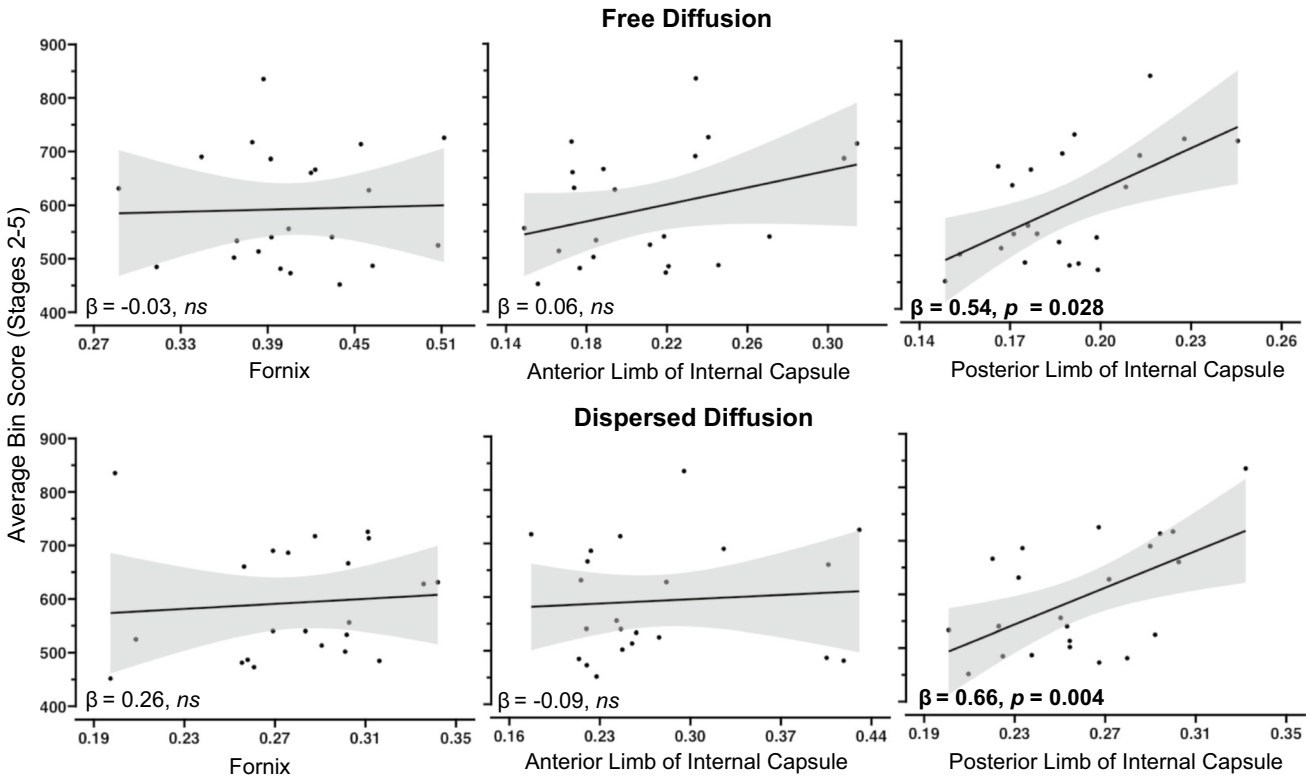

Fig. 4 Associations between white matter microstructure and learning performance. Scatterplots show the significant regression lines and standardized regression coefficients, β, from the multiple linear regression models using free (top) or dispersed (bottom) diffusion to predict bin scores. Results revealed that better microstructure (i.e., lower free and dispersed diffusion) of the posterior limb of the internal capsule significantly predicted better learning (i.e., lower bin scores). The shaded gray area represents 95% confidence intervals.

Table 1 Relationship between associative learning performance and white matter microstructure

	β	*t*(21)	*p*
Dispersion of diffusion			
Fornix	0.26	1.35	0.194
Posterior limb of internal capsule	**0.66**	**3.26**	**0.004**
Anterior limb of internal capsule	-0.09	-0.46	0.649
Free diffusion			
Fornix	-0.03	-0.15	0.886
Posterior limb of internal capsule	**0.54**	**2.39**	**0.028**
Anterior limb of internal capsule	0.06	0.27	0.793
Intracellular diffusion			
Fornix	0.17	0.70	0.493
Posterior limb of internal capsule	-0.39	-1.22	0.237
Anterior limb of internal capsule	0.34	1.03	0.316

Multiple regression analyses testing the effect of white matter microstructure in each region on associative learning performance (average bin score for stages 2-5) are presented separately for each diffusion metric (dispersed, free, intracellular). Significant standardized regression coefficients (β) are bolded.

Discussion

To our knowledge, this study is the first to examine IAL and its underlying white matter microstructural correlates in nonagenarians. We found that the ability to learn associations between cue-cue-target events is evident into the 10th decade of life and is supported by better microstructure of the posterior limb of the internal capsule. Finding that this critical cognitive ability is evident into advanced age and is supported by similar structural neural substrates as seen in younger age groups highlights the importance of the corticostriatal system to learning abilities across the entire lifespan. Given that IAL is important for other higher-level cognitive abilities (e.g., decision making) and everyday activities (e.g., understanding social cues, learning to use new technology), these findings may also implicate IAL as a possible mechanism underlying preserved day-to-day functioning in oldest-old adults without dementia.

Consistent with behavioral evidence of IAL, oldest-old adults had better learning performance during later (Stages 2 through 5) than earlier (Stage 1) task stages. This finding was observed despite participants being unable to describe the regularity between the cues and targets, which is in line

with previous studies using the TLT in younger-old adults (Franco et al., 2021; Howard et al., 2008; Merenstein, Petok, et al., 2021b; Seaman et al., 2014; Stillman, Howard, et al., 2016a; Stillman, Watt, et al., 2016b). Our observation of IAL in the oldest-old may have been facilitated by specific parameters of the TLT version used, including the use of a deterministic regularity, fewer unique triplets, longer presentation times, and increased response time window. An important future direction for this line of work will be to better understand changes in IAL across the lifespan, although this is complicated by limited access to well-characterized oldest-old participants. We also used a rank-ordering binning learning metric with the intention of capturing smaller learning effects that may have been distributed across the dependent measures. Of note, this binning metric was more sensitive to IAL (and white matter microstructure) than the traditional accuracy data (Supplementary Material) and was robust to large variability in the traditional reaction time data (Supplementary Material), possibly resulting from the high prevalence of arthritis in advanced age (Duncan et al., 2011).

As predicted, individual differences in IAL within oldest-old adults were related to differences in the microstructure of cortico-striatal white matter. Specifically, better learning performance (i.e., lower bin scores) was associated with better microstructure (i.e., lower free and dispersed diffusion) of the posterior limb of the internal capsule. These results suggest that individual differences in IAL performance are sensitive to specific microstructural properties in this region, such as the coherence of fiber orientation (dispersed diffusion) or the degree of neurodegeneration and enlargement of perivascular spaces (free diffusion) (Garcia-Hernandez et al., 2022; Sato et al., 2017; Yi et al., 2019). More broadly, the posterior limb of the internal capsule may contribute to the motor learning element of the TLT, as suggested by studies of patients with lesions to this region (Borich et al., 2014; Puig et al., 2011). The posterior limb of the internal capsule also relays neural signals between the basal ganglia (putamen, globus pallidum), thalamus, and motor areas of cortex (Gould & Nolte, 2021). These gray matter regions have previously been implicated in both earlier and later stages of IAL, including our own functional MRI studies using the TLT (Merenstein, Petok, et al., 2021b; Simon et al., 2012). Whereas the posterior limb of the internal capsule is relatively less affected until advanced age (Bennett et al., 2017; Merenstein, Corrada, et al., 2021a), the fornix and anterior limb of the internal capsule remain vulnerable to aging across the older adult lifespan. Thus, microstructure of the latter two tracts may have not related to IAL in the oldest-old due to age-related degradation, although this interpretation will require future studies assessing IAL in both younger-old and oldest-old adults.

Because this is the first investigation of IAL and its white matter correlates in the oldest-old, we considered whether the present findings are in line with the predictions of several neurocognitive aging theories. First, classical cortical disconnection theories derived from patients with neuropsychological disorders propose that cognitive dysfunction arises from disruption to the connections between distributed brain networks (Catani & Ffytche, 2005). Extending these effects of pathology-induced neural disconnection, our finding that better microstructure in a large-scale, white-matter tract relates to better IAL performance supports the notion that white matter microstructure is critical for efficient neurotransmission and ultimately cognitive function among oldest-old adults without dementia (Bennett & Madden, 2014; O'Sullivan et al., 2001). Second, the current observation of IAL, in spite of the high prevalence of dementia-related pathologies (e.g., amyloid-beta and tau neurofibrillary tangles) in this advanced age group, even in those with normal cognition (Kawas et al., 2015), may reflect relatively high levels of brain reserve in older adults living into the 10th decade of life (Stern et al., 2018). Our findings specifically implicate higher cortico-striatal white matter microstructure as a potential form of brain reserve that supports cognitive performance into the 10th decade of life. Although underpowered, this interpretation is further supported by the lack of any significant effect of cognitive status (cognitively impaired no dementia [CIND]) on learning performance or white matter microstructure (data not shown). Finally, finding evidence of IAL in the oldest-old differs from patients with damage to the cortico-striatal loops (e.g., Parkinson's disease), who fail to show evidence of IAL (Meier et al., 2013), and suggests that IAL may be achieved by a relatively more intact cortico-striatal network in advanced aging. For example, better microstructure of the posterior limb of the internal capsule may facilitate the use of compensatory neural activation in motor and striatal gray matter regions, in line with the Scaffolding Theory of Aging and Cognition (Reuter-Lorenz & Park, 2014). However, this interpretation will require future task-related functional MRI studies in the oldest-old, of which there are currently very few (Merenstein & Bennett, 2022).

The present study is strengthened by our examination of the white matter correlates of associative learning, a fundamental yet relatively less studied cognitive process compared to more explicit, fluid domains of cognition and that has been understudied in advanced aging. Our results extend prior work using single-tensor diffusion models in IAL studies of younger-old adults (Bennett et al., 2011) by identifying these relations in an advanced age group and using multicompartment diffusion modelling. Nonetheless, our interpretations will benefit from future studies replicating and extending the current effects of white matter microstructure on IAL within larger samples of nonagenarians and across the entire older adult lifespan. Our examination of these learning effects across participants with normal cognition or CIND increases the generalizability of these findings to the broader oldest-old population, who are often

underrepresented in MRI studies of brain aging. However, additional studies with larger cognitive status subgroups, as well as measurements of dementia-related pathologies, will be necessary to better disentangle the effects of normal versus pathological aging on IAL performance in the oldest-old.

In closing, the ability to learn associations between events is evident in oldest-old adults without dementia and can be attributed to individual differences in microstructural properties of cortico-striatal white matter tracts. Taken together with studies in younger age groups, the current findings underscore the importance of the cortico-striatal network to learning performance across the entire lifespan and suggest that maintaining better microstructure of this network may be especially important for IAL and related cognitive abilities in advanced aging (e.g., decision making, nonverbal communication, skill learning). By demonstrating IAL in advanced age, these results can also inform future interventions aimed at promoting successful aging, such as behavioral and training approaches that capitalize on IAL (repeated exposures, independent of awareness) that may otherwise be futile if this learning ability and its underlying structural network is degraded in advanced age. Ultimately, the current investigation lays important groundwork for future MRI studies of brain and neurocognitive aging in the fastest growing segment of the population (Ferrucci et al., 2008).

Supplementary Information The online version contains supplementary material available at https://doi.org/10.3758/s13415-022-01035-7.

Acknowledgments The authors thank Brooke Jensen, Dana Greenia, and Myra Larson for assistance with data collection and Monique Ramirez for assistance with data quality control. They also thank The 90+ Study participants and their families.

Funding This work was supported by the National Institute of Health: R00 AG047334 to I. J. B., F31 AG071189 to J. L. M., R01 AG053555 to Michael A. Yassa, and R01 AG021055 to C. H. K. and M. M. C.

References

Bennett, I. J., Greenia, D. E., Maillard, P., Sajjadi, S. A., DeCarli, C., Corrada, M. M., & Kawas, C. H. (2017). Age-related white matter integrity differences in oldest-old without dementia. *Neurobiology of Aging, 56*, 108–114. https://doi.org/10.1016/j.neurobiolaging.2017.04.013

Bennett, I. J., Howard, J. H., & Howard, D. V. (2007). Age-related differences in implicit learning of subtle third-order sequential structure. *Journals of Gerontology - Series B Psychological Sciences and Social Sciences, 62*(2). https://doi.org/10.1093/geronb/62.2.P98

Bennett, I. J., & Madden, D. J. (2014). Disconnected aging: Cerebral white matter integrity and age-related differences in cognition. *Neuroscience, 276*, 187–205. https://doi.org/10.1016/j.neuroscience.2013.11.026

Bennett, I. J., Madden, D. J., Vaidya, C. J., Howard, J. H., & Howard, D. V. (2011). White matter integrity correlates of implicit sequence learning in healthy aging. *Neurobiology of Aging, 32*(12), 2317.e1–2317.e12. https://doi.org/10.1016/j.neurobiolaging.2010.03.017

Borich, M. R., Brown, K. E., & Boyd, L. A. (2014). Motor skill learning is associated with diffusion characteristics of white matter in individuals with chronic stroke. *Journal of Neurologic Physical Therapy : JNPT, 38*(3), 151–160. https://doi.org/10.1097/NPT.0B013E3182A3D353

Boyer, M., Destrebecqz, A., & Cleeremans, A. (2005). Processing abstract sequence structure: Learning without knowing, or knowing without learning? *Psychological Research, 69*(5–6), 383–398. https://doi.org/10.1007/s00426-004-0207-4

Brown, C. A., Johnson, N. F., Anderson-Mooney, A. J., Jicha, G. A., Shaw, L. M., Trojanowski, J. Q., Van Eldik, L. J., Schmitt, F. A., Smith, C. D., & Gold, B. T. (2017). Development, validation and application of a new fornix template for studies of aging and preclinical Alzheimer's disease. *NeuroImage : Clinical, 13*, 106. https://doi.org/10.1016/J.NICL.2016.11.024

Catani, M., & Ffytche, D. H. (2005). The rises and falls of disconnection syndromes. *Brain, 128*(Pt 10), 2224–2239. https://doi.org/10.1093/brain/awh622

Cox, R. W. (1996). AFNI: Software for analysis and visualization of functional magnetic resonance neuroimages. *Computers and Biomedical Research, 29*(3), 162–173. https://doi.org/10.1006/cbmr.1996.0014

Curran, T. (1997). Effects of aging on implicit sequence learning: Accounting for sequence structure and explicit knowledge. *Psychological Research, 60*(1–2), 24–41. https://doi.org/10.1007/BF00419678

del Barrio, V. (2004). Diagnostic and statistical manual of mental disorders. *In Encyclopedia of Applied Psychology, Three-Volume Set.* https://doi.org/10.1016/B0-12-657410-3/00457-8

Dennis, N. A., & Cabeza, R. (2011). Age-related dedifferentiation of learning systems: An fMRI study of implicit and explicit learning. *Neurobiology of Aging, 32*(12), 2318.e17–2318.e30. https://doi.org/10.1016/j.neurobiolaging.2010.04.004

Draheim, C., Hicks, K. L., & Engle, R. W. (2016). Combining reaction time and accuracy: The relationship between working memory capacity and task switching as a case example. *Perspectives on Psychological Science, 11*(1), 133–155. https://doi.org/10.1177/1745691615596990

Duncan, R., Francis, R. M., Collerton, J., Davies, K., Jagger, C., Kingston, A., Kirkwood, T., Robinson, L., & Birrell, F. (2011). Prevalence of arthritis and joint pain in the oldest old: Findings from the Newcastle 85+ study. In age and ageing (Vol. 40, issue 6, pp. 752–755). Age ageing. https://doi.org/10.1093/ageing/afr105

Emmenegger, T. M., David, G., Ashtarayeh, M., Fritz, F. J., Ellerbrock, I., Helms, G., Balteau, E., Freund, P., & Mohammadi, S. (2021). The influence of radio-frequency transmit field Inhomogeneities on the accuracy of G-ratio weighted imaging. *Frontiers in Neuroscience, 15*, 770. https://doi.org/10.3389/fnins.2021.674719

Faul, F., Erdfelder, E., Lang, A. G., & Buchner, A. (2007). G*power 3: A flexible statistical power analysis program for the social, behavioral, and biomedical sciences. *Behavior Research Methods, 39*(2), 175–191. https://doi.org/10.3758/BF03193146

Ferrucci, L., Giallauria, F., & Guralnik, J. M. (2008). Epidemiology of aging. *Radiologic Clinics of North America, 46*(4), 643–652. https://doi.org/10.1016/j.rcl.2008.07.005

Folstein, M. F., Folstein, S. E., & McHugh, P. R. (1975). Mini-mental state. *Journal of Psychiatric Research, 12*(3), 189–198. https://doi.org/10.1016/0022-3956(75)90026-6

Franco, C. Y., Petok, J. R., Langley, J., Hu, X., & Bennett, I. J. (2021). Implicit associative learning relates to basal ganglia gray matter microstructure in young and older adults. *Behavioural Brain Research, 397*(July 2020), 112950. https://doi.org/10.1016/j.bbr.2020.112950

Garcia-Hernandez, R., Cerdán Cerdá, A., Trouve Carpena, A., Drakesmith, M., Koller, K., Jones, D. K., Canals, S., & De Santis, S. (2022). Mapping microglia and astrocyte activation in vivo using diffusion MRI. Science. *Advances, 8*(21), eabq2923. https://doi.org/10.1126/SCIADV.ABQ2923/SUPPL_FILE/SCIADV.ABQ2923_SM.PDF

Gould, D. J., & Nolte, J. (2021). *The thalamus and internal capsule: Getting to and from the cerebral cortex. In Nolte's the human brain: An introduction to its functional anatomy* ((8th ed.). ed.). Elsevier.

Graham, J. E., Rockwood, K., Beattie, B. L., Eastwood, R., Gauthier, S., Tuokko, H., & McDowell, I. (1997). Prevalence and severity of cognitive impairment with and without dementia in an elderly population. *Lancet, 349*(9068), 1793–1796. https://doi.org/10.1016/S0140-6736(97)01007-6

Greve, D. N., & Fischl, B. (2009). Accurate and robust brain image alignment using boundary-based registration. *NeuroImage, 48*(1), 63. https://doi.org/10.1016/J.NEUROIMAGE.2009.06.060

Howard, J. H., & Howard, D. V. (2013). Aging mind and brain: Is implicit learning spared in healthy aging? *Frontiers in Psychology, 4*(NOV), 817. https://doi.org/10.3389/fpsyg.2013.00817

Howard, J. H., Howard, D. V., Dennis, N. A., & Kelly, A. J. (2008). Implicit learning of predictive relationships in three-element visual sequences by young and old adults. *Journal of Experimental Psychology: Learning Memory and Cognition, 34*(5), 1139–1157. https://doi.org/10.1037/a0012797

Howard, D. V., Howard, J. H., Japikse, K., DiYanni, C., Thompson, A., & Somberg, R. (2004). Implicit sequence learning: Effects of level of structure, adult age, and extended practice. *Psychology and Aging, 19*(1), 79–92. https://doi.org/10.1037/0882-7974.19.1.79

Hughes, M. M., Linck, J. A., Bowles, A. R., Koeth, J. T., & Bunting, M. F. (2014). Alternatives to switch-cost scoring in the task-switching paradigm: Their reliability and increased validity. *Behavior Research Methods, 46*(3), 702–721. https://doi.org/10.3758/s13428-013-0411-5

Kawas, C., & Corrada, M. (2006). Alzheimers and dementia in the oldest-old: A century of challenges. *Current Alzheimer Research, 3*(5), 411–419. https://doi.org/10.2174/156720506779025233

Kawas, C. H., Kim, R. C., Sonnen, J. A., Bullain, S. S., Trieu, T., & Corrada, M. M. (2015). Multiple pathologies are common and related to dementia in the oldest-old: The 90 + study. *Neurology, 85*(6), 535–542. https://doi.org/10.1212/WNL.0000000000001831

Lieberman, M. D. (2000). Intuition: A social cognitive neuroscience approach. *Psychological Bulletin, 126*(1), 109–137. https://doi.org/10.1037/0033-2909.126.1.109

Meier, B., Weiermann, B., Gutbrod, K., Stephan, M. A., Cock, J., Müri, R. M., & Kaelin-Lang, A. (2013). Implicit task sequence learning in patients with Parkinson's disease, frontal lesions and amnesia: The critical role of fronto-striatal loops. *Neuropsychologia, 51*(14), 3014–3024. https://doi.org/10.1016/J.NEUROPSYCHOLOGIA.2013.10.009

Melazzini, L., Mackay, C. E., Bordin, V., Suri, S., Zsoldos, E., Filippini, N., Mahmood, A., Sundaresan, V., Codari, M., Duff, E., Singh-Manoux, A., Kivimäki, M., Ebmeier, K. P., Jenkinson, M., Sardanelli, F., & Griffanti, L. (2021). White matter hyperintensities classified according to intensity and spatial location reveal specific associations with cognitive performance. *NeuroImage: Clinical, 30*, 102616. https://doi.org/10.1016/j.nicl.2021.102616

Melikyan, Z. A., Corrada, M. M., Dick, M. B., Whittle, C., Paganini-Hill, A., & Kawas, C. H. (2019). Neuropsychological test norms in cognitively intact oldest-old. *Journal of the International Neuropsychological Society : JINS, 25*(5), 530–545. https://doi.org/10.1017/S1355617719000122

Merenstein, J. L., & Bennett, I. J. (2022). Bridging patterns of neurocognitive aging across the older adult lifespan. *Neuroscience and Biobehavioral Reviews, 135*(November 2021), 104594. https://doi.org/10.1016/j.neubiorev.2022.104594

Merenstein, J. L., Corrada, M. M., Kawas, C. H., & Bennett, I. J. (2021a). Age affects white matter microstructure and episodic memory across the older adult lifespan. *Neurobiology of Aging, 106*, 282–291. https://doi.org/10.1016/j.neurobiolaging.2021.06.021

Merenstein, J. L., Petok, J. R., & Bennett, I. J. (2021b). Age group differences in learning-related activity reflect task stage, not learning stage. *Behavioural Brain Research, 416*(September 2021), 113570. https://doi.org/10.1016/j.bbr.2021.113570

Mori, S., Oishi, K., Jiang, H., Jiang, L., Li, X., Akhter, K., Hua, K., Faria, A. V., Mahmood, A., Woods, R., Toga, A. W., Pike, G. B., Neto, P. R., Evans, A., Zhang, J., Huang, H., Miller, M. I., van Zijl, P., & Mazziotta, J. (2008). Stereotaxic white matter atlas based on diffusion tensor imaging in an ICBM template. *NeuroImage, 40*(2), 570–582. https://doi.org/10.1016/j.neuroimage.2007.12.035

O'Sullivan, M., Jones, D. K., Summers, P. E., Morris, R. G., Williams, S. C. R., & Markus, H. S. (2001). Evidence for cortical "disconnection" as a mechanism of age-related cognitive decline. *Neurology, 57*(4), 632–638. https://doi.org/10.1212/WNL.57.4.632

Puig, J., Pedraza, S., Blasco, G., Daunis-i-Estadella, J., Prados, F., Remollo, S., Prats-Galino, A., Soria, G., Boada, I., Castellanos, M., & Serena, J. (2011). Acute damage to the posterior limb of the internal capsule on diffusion tensor Tractography as an early imaging predictor of motor outcome after stroke. *American Journal of Neuroradiology, 32*(5), 857–863. https://doi.org/10.3174/AJNR.A2400

Reuter-Lorenz, P. A., & Park, D. C. (2014). How does it STAC up? Revisiting the scaffolding theory of aging and cognition. *Neuropsychology Review, 24*(3), 355–370. https://doi.org/10.1007/s11065-014-9270-9

Rieckmann, A., Fischer, H., & Bäckman, L. (2010). Activation in striatum and medial temporal lobe during sequence learning in younger and older adults: Relations to performance. *NeuroImage, 50*(3), 1303–1312. https://doi.org/10.1016/j.neuroimage.2010.01.015

Sato, K., Kerever, A., Kamagata, K., Tsuruta, K., Irie, R., Tagawa, K., Okazawa, H., Arikawa-Hirasawa, E., Nitta, N., Aoki, I., & Aoki, S. (2017). Understanding microstructure of the brain by comparison of neurite orientation dispersion and density imaging (NODDI) with transparent mouse brain. *Acta Radiologica Open, 6*(4), 2058460117703816. https://doi.org/10.1177/2058460117703816

Seaman, K. L., Howard, D. V., & Howard, J. H. (2014). Adult age differences in learning on a sequentially cued prediction task. *The Journals of Gerontology Series B: Psychological Sciences and Social Sciences, 69*(5), 686–694. https://doi.org/10.1093/geronb/gbt057

Seger, C. A. (1994). Implicit learning. *Psychological Bulletin, 115*(2), 163–196. https://doi.org/10.1037/0033-2909.115.2.163

Simon Jr., J. R., Howard Jr., J. H., & Howard, D. V. (2010). Age differences in implicit learning of probabilistic unstructured sequences. *The Journals of Gerontology: Series B, 66B*(1), 32–38. https://doi.org/10.1093/GERONB

Simon, J. R., Vaidya, C. J., Howard, J. H., & Howard, D. V. (2012). The effects of aging on the neural basis of implicit associative learning in a probabilistic triplets learning task. *Journal of Cognitive Neuroscience, 24*(2), 451–463. https://doi.org/10.1162/jocn_a_00116

Stern, Y., Arenaza-Urquijo, E. M., Bartrés-Faz, D., Belleville, S., Cantilon, M., Chetelat, G., Ewers, M., Franzmeier, N., Kempermann, G., Kremen, W. S., Okonkwo, O., Scarmeas, N., Soldan, A., Udeh-Momoh, C., Valenzuela, M., Vemuri, P., Vuoksimaa, E., Arenaza Urquiljo, E. M., Bartrés-Faz, D., & Vuoksimaa, E. (2018). Whitepaper: Defining and investigating cognitive reserve, brain reserve, and brain maintenance. *Alzheimer's & Dementia.* https://doi.org/10.1016/J.JALZ.2018.07.219

Stillman, C. M., Howard, J. H., & Howard, D. V. (2016a). The effects of structural complexity on age-related deficits in implicit probabilistic sequence learning. *Journals of Gerontology - Series B Psychological Sciences and Social Sciences, 71*(2), 212–219. https://doi.org/10.1093/geronb/gbu135

Stillman, C. M., Watt, J. C., Grove, G. A., Wollam, M. E., Uyar, F., Mataro, M., Cohen, N. J., Howard, D. V., Howard, J. H., & Erickson, K. I. (2016b). Physical activity is associated with reduced implicit learning but enhanced relational memory and executive functioning in young adults. *PLoS One, 11*(9), e0162100. https://doi.org/10.1371/journal.pone.0162100

Stillman, C. M., You, X., Seaman, K. L., Vaidya, C. J., Howard, J. H., & Howard, D. V. (2016c). Task-related functional connectivity of the caudate mediates the association between trait mindfulness and implicit learning in older adults. *Cognitive, Affective, & Behavioral Neuroscience, 16*(4), 736–753. https://doi.org/10.3758/s13415-016-0427-2

Wakana, S., Jiang, H., Nagae-Poetscher, L. M., Van Zijl, P. C. M., & Mori, S. (2004). Fiber tract-based atlas of human white matter anatomy. *Radiology, 230*(1), 77–87. https://doi.org/10.1148/radiol.2301021640

Wycoco, V., Shroff, M., Sudhakar, S., & Lee, W. (2013). White matter anatomy. What the radiologist needs to know. *Neuroimaging Clinics of North America, 23*(2), 197–216. https://doi.org/10.1016/j.nic.2012.12.002

Yi, S. Y., Barnett, B. R., Torres-Velázquez, M., Zhang, Y., Hurley, S. A., Rowley, P. A., Hernando, D., & Yu, J. P. J. (2019). Detecting microglial density with quantitative multi-compartment diffusion MRI. *Frontiers in Neuroscience, 13*(FEB), 81. https://doi.org/10.3389/FNINS.2019.00081/BIBTEX

Zhang, H., Schneider, T., Wheeler-Kingshott, C. A., & Alexander, D. C. (2012). NODDI: Practical in vivo neurite orientation dispersion and density imaging of the human brain. *NeuroImage, 61*(4), 1000–1016. https://doi.org/10.1016/j.neuroimage.2012.03.072

Zhang, Y., Brady, M., & Smith, S. (2001). Segmentation of brain MR images through a hidden Markov random field model and the expectation-maximization algorithm. *IEEE Transactions on Medical Imaging, 20*(1), 45–57. https://doi.org/10.1109/42.906424

Open Practices Statement This study was not preregistered. The data that support the findings of this study are available from the corresponding author, J. L. M., upon request.